frontiers | Frontiers in Earth Science

TYPE Original Research
PUBLISHED 12 January 2023
DOI 10.3389/feart.2022.1025231

OPEN ACCESS

EDITED BY
Zizheng Guo,
Hebei University of Technology, China

REVIEWED BY
Emad Elhout,
Pharos University in Alexandria, Egypt
Yuhang Zhu,
China University of Geosciences Wuhan, China

*CORRESPONDENCE
Dewen Liu,
civil_liudewen@sina.com

SPECIALTY SECTION
This article was submitted to Geohazards and Georisks, a section of the journal Frontiers in Earth Science

RECEIVED 22 August 2022
ACCEPTED 31 October 2022
PUBLISHED 12 January 2023

CITATION
Shu T, Li Q, Wang T, Jiang L, Guo Z, Lei M and Liu D (2023), Study on the shock-absorbing effect of a new staggered story isolated structure under the long-period earthquake motion.
Front. Earth Sci. 10:1025231.
doi: 10.3389/feart.2022.1025231

Study on the shock-absorbing effect of a new staggered story isolated structure under the long-period earthquake motion

Tong Shu[1], Qi Li[1], Taize Wang[1], Luwei Jiang[2], Zhongfa Guo[3], Min Lei[4] and Dewen Liu[1]*

[1]College of Civil Engineering, Southwest Forestry University, Kunming, China, [2]Yunnan Communications Vocational and Technical College, Kunming, China, [3]Shandong Jining Wenshang County Architectural Design Institute Co., Ltd, Jining, China, [4]College of Civil Engineering, Southwest Jiaotong University, Chengdu, China

The finite element model of a new staggered story isolated structure is established. Using the time-history analysis method, the dynamic response state of the structure at each time step is calculated by integrating the acceleration time-history data step-by-step. Three different types of seismic waves (ordinary seismic wave, near-fault impulse seismic wave, far-field quasi harmonic and long-period seismic wave) are input respectively for dynamic time history analysis. The result indicates that the new staggered story isolated structure has a good shock absorption effect under the action of three different types of seismic waves. There are certain differences in the shock absorption effect under the three kinds of ground motions. The seismic response under ordinary ground motions is minimal, but the seismic response of the structure increases in response to far-field quasi harmonic and long-period ground motions and the near-field fault pulse ground motions. Meanwhile, the inter-story shear force, inter story acceleration, inter-story displacement, damage, and the energy input are all increasing, However, compared with the aseismic structure, the inter-story shear force is reduced by 48%, the inter-story acceleration is reduced by 23%, the inter-story displacement is reduced by 48%, and the energy dissipation rate of the isolated layer is 65%. In addition, the isolated bearing is in good condition during occasional earthquakes under normal ground motion. However, the bearing exceeds the permissible range during near-fault impulse ground motion and far-field harmonic and long-period earthquakes. Therefore, special consideration should be given to the area where the far-field harmonic and long-period ground motion are involved.

KEYWORDS

new staggered story isolated structure, long period earthquake, finite element analysis, earthquake response, shock absorption performance

1 Introduction

In recent years, the new staggered story isolated structure, a new form of isolated structure built on the basis of the base isolated and mid-story isolated systems, has become one of the research hotspots in the field of disaster prevention and mitigation. The isolated layer of the base isolated structure and the mid-story isolated structure is positioned on a specific structure layer. Different from the above two kinds of isolated systems, the isolated story of the new staggered story isolated structure is divided into two parts. The isolated story of core tube part is located at the bottom of the core tube, forming a similar to base isolated mode, the isolated story of the frame part is located in the middle of the structure, forming a similar to mid-story isolated mode. However, the isolated layer of the new staggered mid-story isolated structure is located on different layers of the structure (Liu et al., 2022; Zhang et al., 2022). The new staggered story isolated structure has been implemented in practical projects. For instance, after the Istanbul earthquake, a hospital was strengthened with a new staggered story isolated structure (Erdik et al., 2018).

It is known to all that earthquakes occur frequently all over the world. Therefore, the research on isolated structures has been increasing. The base isolated structure has experienced three developments, each of which is an important improvement (De Luca and Guidi, 2019). The base isolated structure can successfully safeguard buildings during powerful earthquakes (Losanno et al., 2021) and lessen the seismic response of structures (Cancellara and De Angelis, 2016; Hayashi et al., 2018; Park and Ok, 2021; Pérez-Rocha et al., 2021; Qahir Darwish and Bhandari, 2022; Clemente et al., 2021). Jose et al. (2021) compared and evaluated the response of the aseismic structure and the base isolated structure under earthquakes, and demonstrated that the structure had a strong shock absorption effect when using the base-isolated structure. In addition, researchers have researched a range of isolated bearings and discovered that most isolated bearings cannot only reduce the inter-story shear force and inter-story acceleration of the structure, but also control the displacement of the isolated layer of the structure (Castaldo and Tubaldi, 2018; Fu et al., 2019; Shan et al., 2020; Shang and Hu, 2020; Forcellini and Gallanti, 2018). Various isolated bearings have various damping effects on the structure, which can effectively reduce the earthquake response (Behzad Talaeitaba et al., 2021; Van-Thuyet, 2021; Ali et al., 2022; Wu et al., 2022). Recently, Öncü-Davas (2022) has investigated the optimization of a nonlinear foundation isolated system under near-fault earthquakes. Rostami (2021) investigated the lateral load distribution of static analysis of the base isolated building frames subject to far-fault and near-fault ground motions through three scaling methods. It is found that the inter-story shear force of the structure will be underestimated, and the lateral force formula of the LRBs base-isolated structure is determined. Kamble (2022) discovered that the base-isolated structure under three-dimensional ground motion had a favorable effect on shock absorption. The findings of the study show that significant reduction in the lateral displacement and acceleration of the S-system is achieved by base isolating the building. In addition, the S-system's vertical responses are reduced despite the isolated being ineffective in the vertical direction. The method of machine learning has significance for the research of seismic isolated, and it has a high sensitivity rate prediction accuracy to put forward the early warning of disaster. (Guo et al., 2022a; Chang et al., 2022). Guo et al. (2022b) used numerical simulation method to effectively study how to solve the disaster under different circumstances.

The development of the base isolated structure has taken a long period, and it has been widely used all over the world. However, the adaptability of a mid-story isolated structure is greater than that of a base isolated structure (Li et al., 2022). However, the development period for a mid-story isolated structure is relatively short, and thus the research is relatively insufficient. Therefore, Zhang (Liu et al., 2021) suggested a semi-analytical solution of mid-story isolated structural system considering the bending deformation and shear deformation of the structure. In addition, Chang and Zhu (2011) discovered that both the superstructure and the substructure have good shock absorption effect (Loh et al., 2013). Liu et al. (2018) discovered that viscous fluid dampers can effectively enhance the seismic performance of mid-story isolated structures. Moreover, the application of mid-story isolated structure in the reinforcement of existing structures can effectively lower the seismic response of structures (Li et al., 2014; Faiella et al., 2020; Ma et al., 2020; Saha and Mishra, 2021; Hur and Park, 2022). Use machine learning methods to predict the occurrence of disasters in different environments. (Huang et al., 2020a; Huang et al., 2020b; Huang et al., 2020c).

Because the period of the isolated structure is extended, it is easy to generate a substantial seismic response as a result of resonance under the action of long-term ground motion. Liao et al. (2001) utilized the ratio of peak ground motion velocity to peak acceleration (PGV/PGA) to determine whether the ground motion is long-term ground motion, and studied the seismic response of 5-story and 12-story frame structures under near-field long-term ground motion and ordinary ground motion. The results show that the near-fault earthquake results in much more damage than the far-field earthquake. In addition, Minagawa and Fujita (2006) and other researchers discovered that the natural vibration period of the structural system was prolonged by setting the isolated layer, but increased the seismic response was larger under long-period ground motion. Cheng et al. (2021) investigated the seismic energy response of two typical long-period ground motion single degree of freedom (SDOF) systems. In addition, Zhou et al. (2018) investigated the distinction between the absolute acceleration spectrum and the pseudo acceleration spectrum based on the hysteretic restoring

force of the structure, as well as the pseudo acceleration spectrum of long-period earthquake. Moreover, Hu et al. (2018) proposed a three segment curve model that combines the calibrated seismic factors with a random simulation program, and verified it by comparing it to the seismic simulation. (Guo et al., 2021); Huang et al. (2022) improved the accuracy of disaster prediction, use machine learning methods to predict and monitor the occurrence of disasters (Jiang et al., 2018; Chang et al., 2020). (Pytel et al. (2016) studied the influence of different factors on seismic activity. Mashinskii (2019) studied the unusual behavior of rock inelasticity, thereby deepening the understanding of the propagation and attenuation of seismic waves in the real environment.

According to the above analysis, at present, most of research focus on the base isolated structure and the mid-story isolated structure. However, there are fewer studies on the new staggered story isolated structure. In addition, previous research mainly focus on the seismic response of isolated structures during conventional earthquakes, while the impact of long-period ground motions has received less attention. Furthermore, compared to ordinary ground motions, the damage caused by long-period periodic ground motions to high-rise buildings with a large natural vibration period is more severe. But in China's seismic code design, there is no provision for controlling the damage caused by long-period ground motions to high-rise structures. Therefore, it is of great significance to examine the seismic response of the new staggered story isolated structure under long-period ground motions.

In this paper, the seismic response of a new staggered story isolated structure under ordinary ground motion, near-fault impulse ground motion, and far-field harmonic long-period ground motion is studied. The damping effect, structural damage, structural energy consumption, and the response findings of the isolated bearing of the innovative staggered story isolated structure under three different ground motions are obtained. It is expected to provide a reference for the design and research of the new staggered story isolated structure.

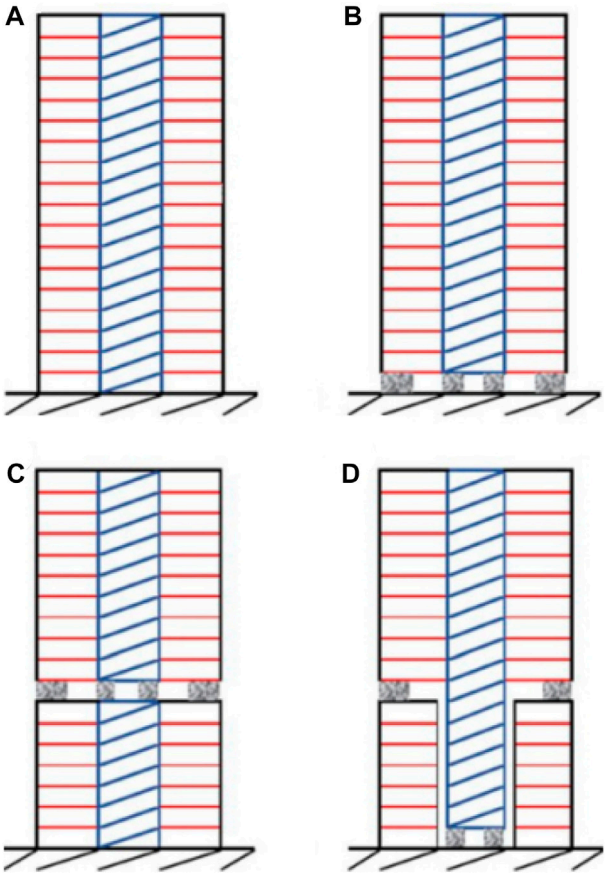

FIGURE 1
Structure diagram: **(A)** aseismic structure, **(B)** base isolated structure, **(C)** mid-story isolated structure, **(D)** new staggered story isolated structure (The blue part represents the core tube, the red part represents the frame, and the shadow part represents the isolated bearings).

2 Materials and methods

2.1 Project overview

The seismic fortification grade of a new staggered story isolated structure is class B with the seismic fortification intensity of 8°. The basic seismic acceleration is designed as 0.20 g, and the seismic group is designed as group II. The building site is defined as class III. The building, whose plane size is 26 m × 26 m, with 20 floors in total, adopts frame-core tube structure, and a floor height of 3 m. The frame isolated layer is positioned on the third level of the frame structure, whereas the middle core tube is located at the bottom of the core tube. Figure 1 compares the aseismic structure, the base isolated structure, the mid-story isolated structure, and the new staggered story isolated structure. Figure 2 depicts the three-dimensional finite element model of the structure. The sectional dimensions of the structure can be seen in Table 1. The concrete strength of the frame column and beam is C40, and all reinforcement models are HRB400. The thickness of the concrete cover is 50 mm. Shear walls are simulated by thin-shell elements with a concrete thickness of 250 mm.

2.2 Modeling

The finite element analysis software ETABS is utilized to assess the isolated design of frame core tube structure. Extract the column bottom reaction at the isolated bearing under the

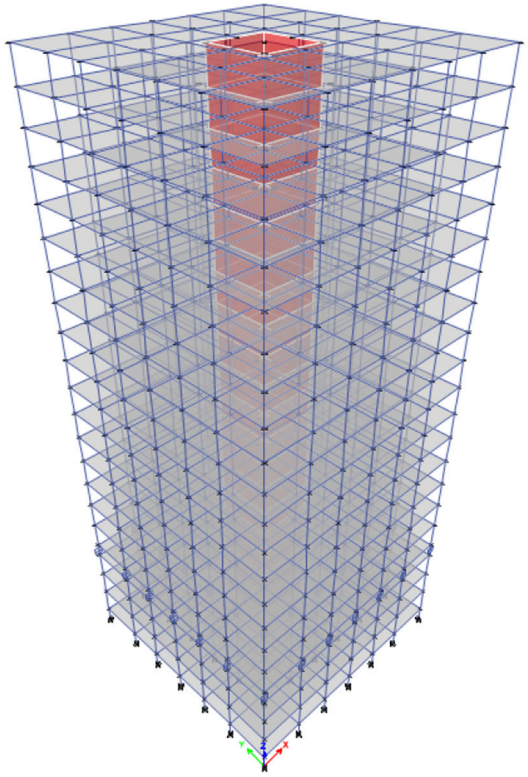

FIGURE 2
3D diagram of new staggered story isolated structure.

working condition of standard value of gravity load using the ETABS software, and estimate the number and model of isolated bearings according to the total horizontal yield force being 2% of the column bottom reaction under standard value of gravity load. LRB1000 is utilized for the core tube, while LRB600 is used for the frame. The parameters of isolated bearings are provided in Table 2 below, and their arrangement is depicted in Figure 3.

2.3 Earthquake wave selection

The seismic fortification intensity is set to degree 8, and the basic acceleration value of the earthquake is set to 0.2 g. Meanwhile, the site category is class 2, and the seismic group is designed as group III. The ground motion criteria are selected as follows: the average period of ground motion acceleration spectrum Tr and PGV/PGA values are used as the basis for distinguishing ordinary ground motion from long-period ground motion. When Tr >2 s and PGV/PGA>0.2, it is long-period ground motion, otherwise it is ordinary ground motion. Table 3 contains information regarding the selected near-fault impulse ground motion, the far-field harmonic long-period ground motion, and the ordinary ground motion.

Each of the three types of ground motion have unique characteristics. Figure 4 depicts the acceleration response spectrum of ground motion and illustrates that the peak value of the acceleration spectrum of ordinary ground motion occurs between 0.3 s and 0.4 s, and that when the structural period is about 2 s, the acceleration spectrum value is less than 10%–20% of the peak value. The spectrum of the near-fault impulse ground motion acceleration response is essentially identical to the spectrum of the ordinary ground motion acceleration response. When the structural period is greater than 2 s, the peak value of the near-fault impulse ground motion acceleration response spectrum is greater than that of the ordinary ground motion acceleration response spectrum.

The acceleration response spectrum of the far-field harmonic like long-period ground motion differs significantly from that of the other two ground motions. Due to the appearance of harmonic like components, the acceleration spectrum of the far-field harmonic like long-period ground motion would reach its maximum value between 3 and 6 s during the structural period, resulting in an obvious "double peak" phenomenon. The near-fault impulse ground motion and the far-field harmonic long-period ground motion have a greater impact on long-period structures, which requires special consideration.

TABLE 1 Frame section parameters.

Component type	Component location/Layer	Section size	
		Height/mm	Width/mm
Framed Column	1–20	800	800
Framed Column	1–20	700	350

TABLE 2 Parameters of isolated bearing.

Model	Effective diameter/mm	Total rubber thickness/mm	Total stiffness before yield/kN•m	Equivalent stiffness		Vertical stiffness/kN•mm	Yield force/kN
				100% horizontal shear deformation/kN•m	250% horizontal shear deformation/kN•m		
LRB600	600	112	16.39	1.83	1.83	2,200	63
LRB1000	1,000	186	27.08	3.19	3.19	4,300	203

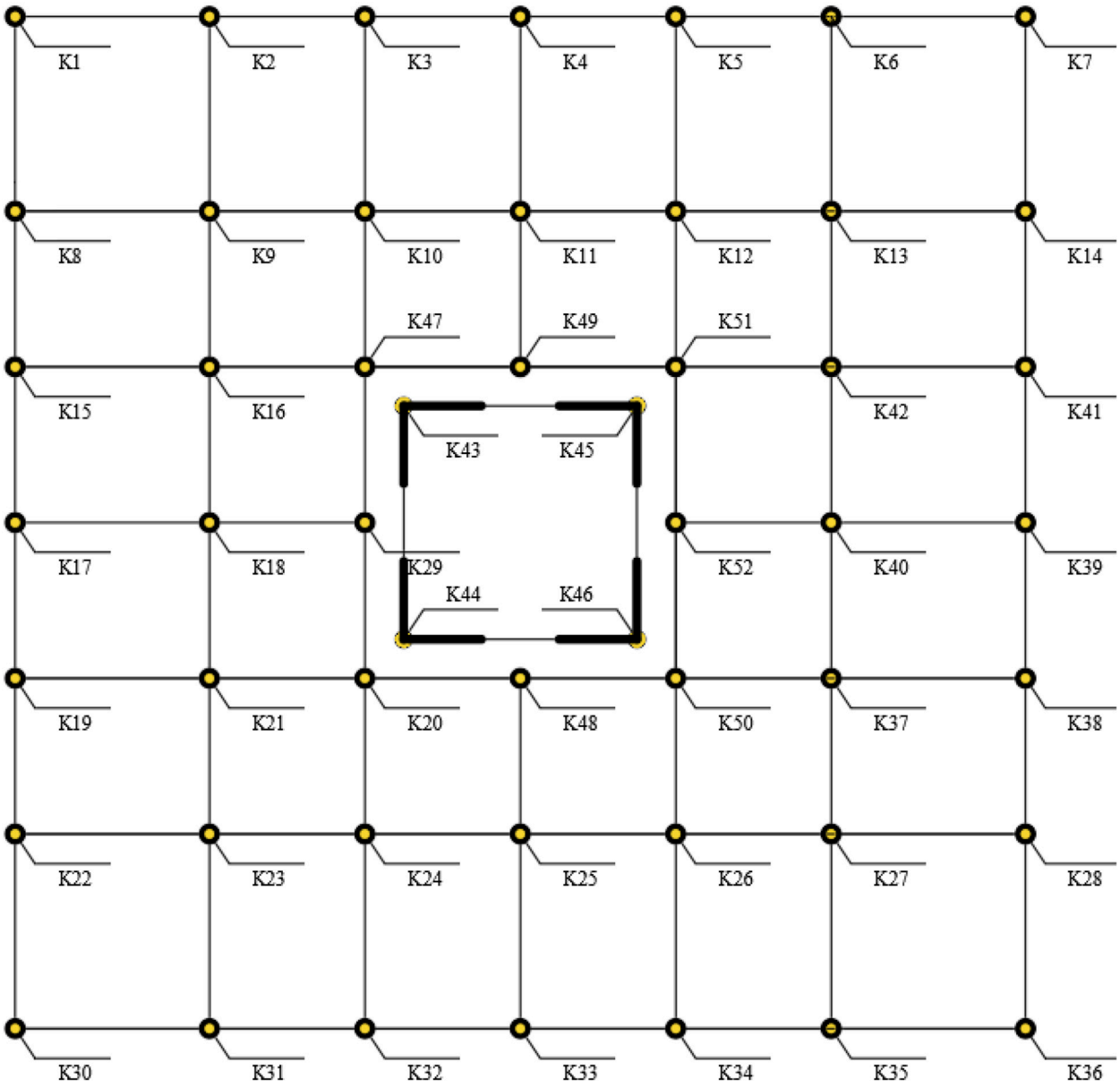

FIGURE 3
Layout of isolated bearing.

TABLE 3 Basic information of three types of earthquake motion.

Earthquake records	Station	Earthquake magnitude	Epicentral distance (km)	PGV/PGA
Normal ground motion records	Bolu	7.14	12.04	0.12
	Artificial wave	—	—	—
Near-fault pulse-like ground motions	Chi-Chi TCU036	7.62	19.83	0.43
	Chi-Chi TCU063	7.62	9.78	0.24
	Chi-Chi TCU054	7.62	5.28	0.21
	Chi-Chi TCU102	7.62	1.49	0.31
	Chi-Chi TCU122	7.62	9.34	0.20
	Chi-Chi TCU044	6.2	62.87	0.22
	Chi-Chi TCU039	7.62	19.89	0.28
Far-field harmonic like long-period ground motion	Chi-Chi CHY093	7.62	49.82	0.27
	Chi-Chi ILA056	7.62	92.04	0.48
	Chi-Chi ILA048	7.62	86.67	0.35
	Chi-Chi TCU140	7.62	32.95	0.28
	Chi-Chi CHY092	7.62	22.69	0.26
	Chi-Chi CHY082	7.62	36.09	0.33
	Chi-Chi TCU006	7.62	72.52	0.24

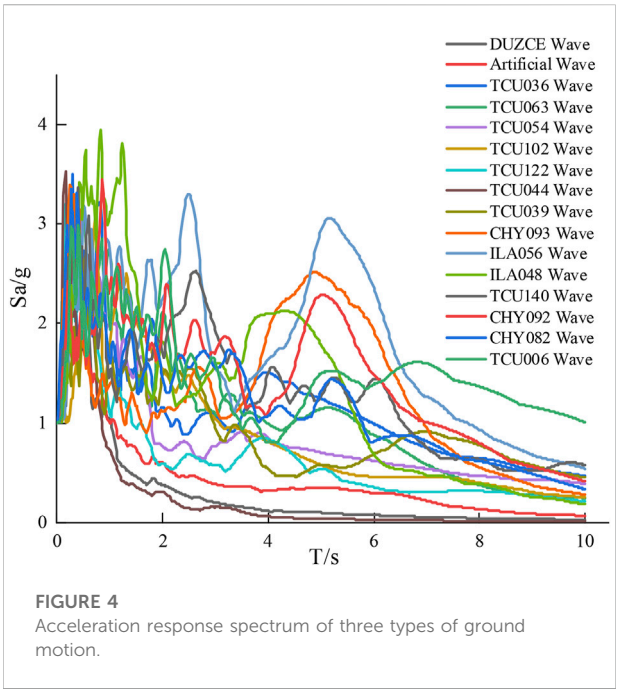

FIGURE 4
Acceleration response spectrum of three types of ground motion.

3 Analysis of the shock absorption effect

3.1 Structural seismic response

The finite element models of the aseismic structure and a new staggered story isolated structure are developed. By integrating acceleration time-history data at each time step, the time-history analysis approach determines the dynamic response state of the structure at each time step. Three different types of seismic waves (ordinary seismic wave, near-fault impulse seismic wave, far-field quasi harmonic and long-period seismic wave) are input respectively for dynamic time history analysis under 8° moderate earthquake (peak acceleration of 20 0cm/s2). Under three earthquake motions, the seismic response, energy dissipation, and structural damage of a new staggered story isolated structure are determined.

3.1.1 Modal period

Table 4 compares the results of the first three modal periods for the aseismic structure and the new staggered story isolated structure. It can be seen from Table 4 that the period of the first three steps of the new staggered story isolated structure is greater than that of the aseismic structure.

Before isolated, the fundamental period of the structure is 1.069 s, while after isolated, the basic period of the structure is 2.434 s. It is a structure with a long natural vibration period and a significant response to a long-period earthquake. Therefore, it is necessary to select the long-period seismic wave for nonlinear time history analysis and compare it to nonlinear time history analysis under ordinary seismic wave.

3.1.2 Basal shear force

The finite element models of the aseismic structure and the new staggered story isolated structure are developed. Three different types of seismic waves (ordinary seismic wave, near-fault impulse seismic wave, far-field quasi harmonic and long-period seismic wave) are input respectively for dynamic time history analysis under 8° moderate earthquake (peak acceleration of 200 cm/s2).

TABLE 4 The first three modal periods of aseismic structures and new staggered story isolated structures.

Type of construction	First cycle/s	Second cycle/s	Third cycle/s
Aseismic structure	1.069	1.069	0.983
New staggered story isolated structure	2.434	2.434	2.286

TABLE 5 Energy consumption of new staggered story isolated structure.

Type of construction	Earthquake wave	Total seismic input energy (KN·m)	Self damping energy dissipation of structure (KN·m)	Energy consumption of isolated layer (KN·m)	Energy consumption rate of isolated layer (%)	Average decreasing amplitude ratio (%)
New staggered story isolated structure	TCU036	30,237.38	8,861.04	21,375.39	70.69	65.33
	TCU063	56,677.06	19,684.67	36,989.24	65.26	
	TCU054	19,262.63	5,340.15	13,910.95	72.21	
	TCU102	96,753.67	48,996.79	47,749.78	49.35	
	TCU122	11,187.72	3,272.20	7,907.86	70.68	
	TCU044	2,448.45	1,114.83	1,330.60	54.34	
	TCU039	30,456.48	9,113.52	21,339.78	70.07	
	ILA056	96,620.43	40,033.61	56,558.64	58.54	
	CHY093	34,496.03	8,353.70	26,034.44	75.47	
	ILA048	52,257.12	16,193.48	36,039.96	58.97	
	TCU140	106,048.22	39,201.59	66,775.30	62.97	
	CHY092	87,257.79	31,396.49	55,833.21	63.99	
	CHY082	38,920.69	11,933.08	26,924.01	69.18	
	TCU006	47,461.00	14,900.38	32,549.80	68.58	
	DUZCE	2,311.63	837.65	1,473.51	63.74	
	Artificial wave	6,213.85	1780.70	4,429.15	71.28	

Table 5 depicts the base shear force comparison between the new staggered story isolated structure and the aseismic structure. Figure 5 demonstrates that, compared to the aseismic structure, the base shear force of the new staggered story isolated structure is reduced under three different types of earthquakes, but not under some long-period seismic waves.

3.1.3 Inter-laminar shear force

Figure 6 depicts a comparison of the story shear force between the new staggered story isolated structure and the non-isolated structure under the action of three different types of seismic waves (ordinary seismic wave, near-fault impulse seismic wave, far-field harmonic and long-period seismic wave). Figure 6 demonstrates that the new staggered story isolated structure has a damping effect under the action of three different types of earthquakes, and that the isolated effect of the core tube below the frame isolated layer of the new staggered story isolated structure is superior to that of the frame. The seismic response of aseismic structures in the

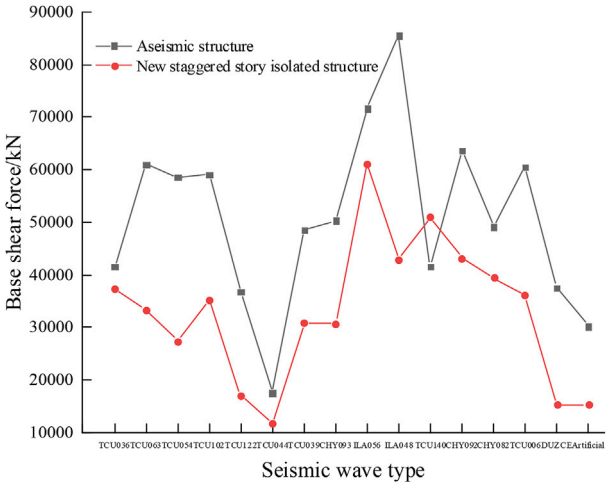

FIGURE 5
Comparisons of base shear force between the aseismic structure and the new staggered story isolated structure.

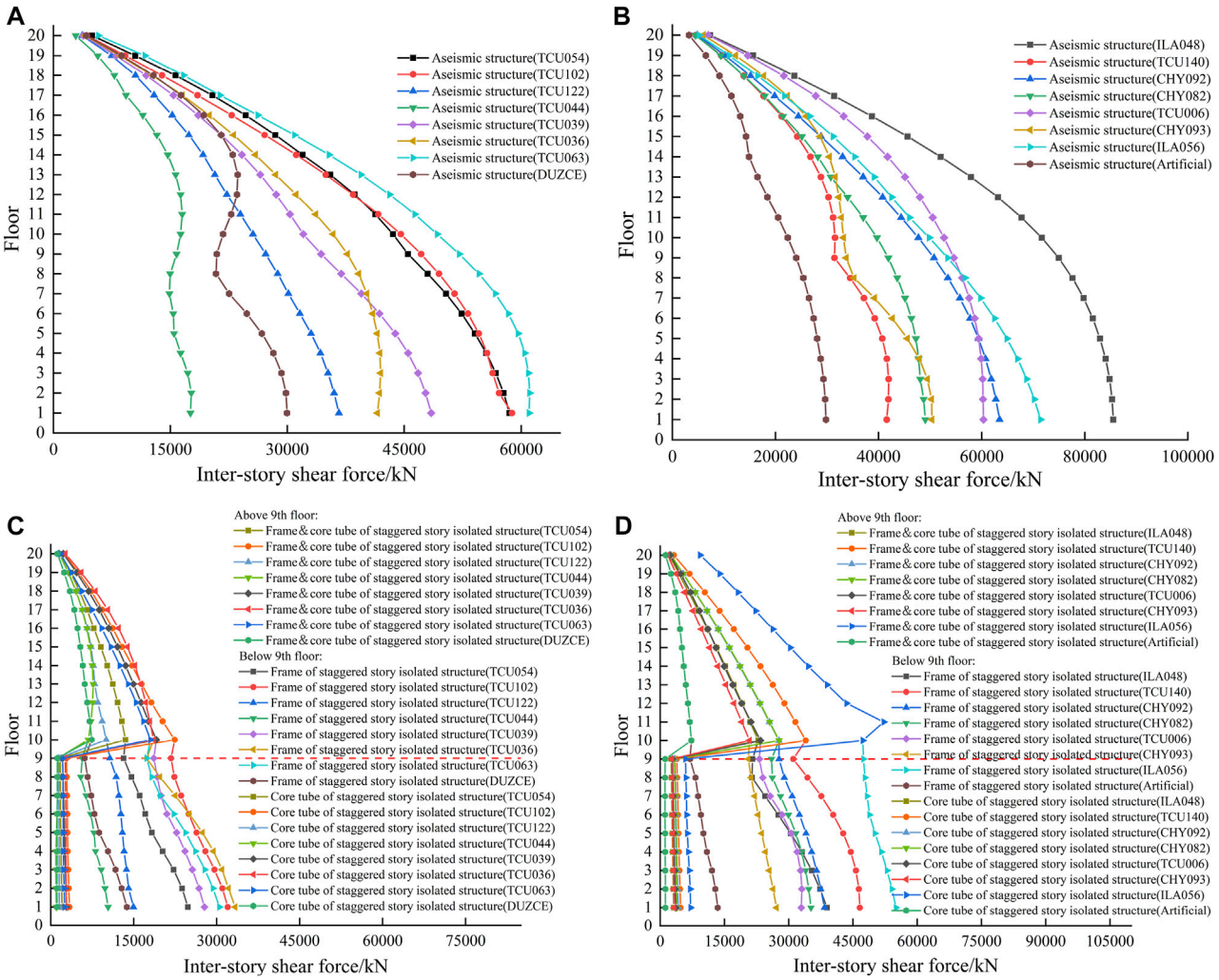

FIGURE 6
Comparisons of inter-story shear force between aseismic structure and new staggered story isolated structure: **(A)** comparison of inter-story shear force of aseismic structure under near-fault pulse-like ground motion **(B)** comparison of inter-story shear force of aseismic structure under far-field harmonic like long-period ground motion, **(C)**comparison of inter-story shear force of new staggered story isolated structure under near-fault pulse-like ground motion, and **(D)** comparison of inter-story shear force of new staggered story isolated structure under far-field harmonic like long-period ground motion.

presence of far-field harmonic long-period ground motion and near-fault impulse ground motion is greater than that of ordinary ground motion. The seismic response of the new staggered story isolated structure under far-field harmonic long-period ground motion and near-fault impulse ground motion is greater than that of the ordinary ground motion. Compared with the aseismic structure, the story shear force of the new staggered story isolated structure is reduced, and the shear force of the frame below the frame isolated layer is more than that of the core tube. During the far-field harmonic long-period ground motion, the inter-laminar shear force is greater than that under the near-fault pulse long-period ground motion.

3.1.4 Inter layer acceleration

Figure 7 illustrates the comparison of story accelerations between the new staggered story isolated structure and the aseismic structure under the action of three different types of seismic waves (ordinary seismic wave, near-fault impulse seismic wave, far-field harmonic and long-period seismic wave). According to Figure 7, the new staggered story isolated structure has certain damping effect under the action of three types of earthquakes. In the new staggered-story isolated

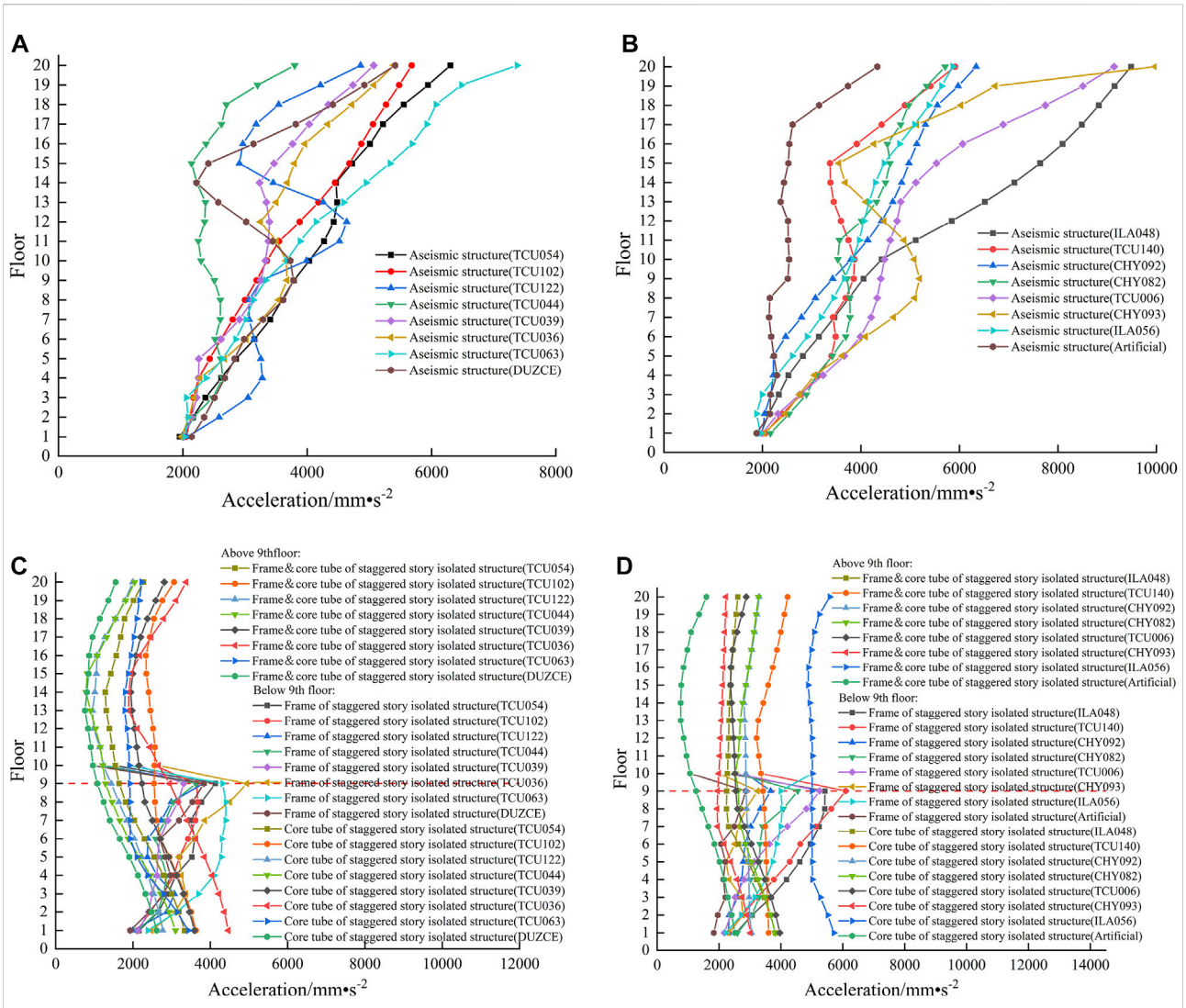

FIGURE 7
Comparisons of story acceleration between aseismic structure and new staggered story isolated structure: **(A)** acceleration comparison of aseismic structure under near-fault pulse-like ground motion **(B)** acceleration comparison of aseismic structure under far-field harmonic like long-period ground motion, **(C)** acceleration comparison of new staggered story isolated structure under near-fault pulse-like ground motion, and **(D)** acceleration comparison of new staggered story isolated structure under far-field harmonic like long-period ground motion.

structure, the acceleration of the core tube beneath the frame-isolated layer is greater than that of the frame part. Under the action of far-field harmonic long-period ground motion and near-fault impulse ground motion, the accelerations of the frame part and the core tube part under the frame isolated layer of the new staggered story isolated structure are greater than those of the aseismic structure. The seismic response of aseismic structures in the presence of the far-field harmonic long-period ground motion and near-fault impulse ground motion is greater than that of the ordinary ground motion. The seismic response of the new staggered story isolated structure under the far-field harmonic long-period ground motion and near-fault impulse ground motion is greater than that of the ordinary ground motion. Among them, the inter-layer acceleration under the far-field harmonic long-period ground motion is greater than that under the near-fault pulse long-period ground motion.

3.1.5 Story displacement

Figure 8 depicts a comparison of the story displacement between the new staggered story isolated structure and the aseismic structure under the influence of three distinct types of seismic waves (ordinary seismic wave, near-fault impulse seismic wave, far-field harmonic and long-period seismic wave). Figure 8 demonstrates that under the influence of three types of earthquakes, the new staggered story isolated structure has a certain damping effect. In the new staggered story isolated structure, the displacement of the core tube

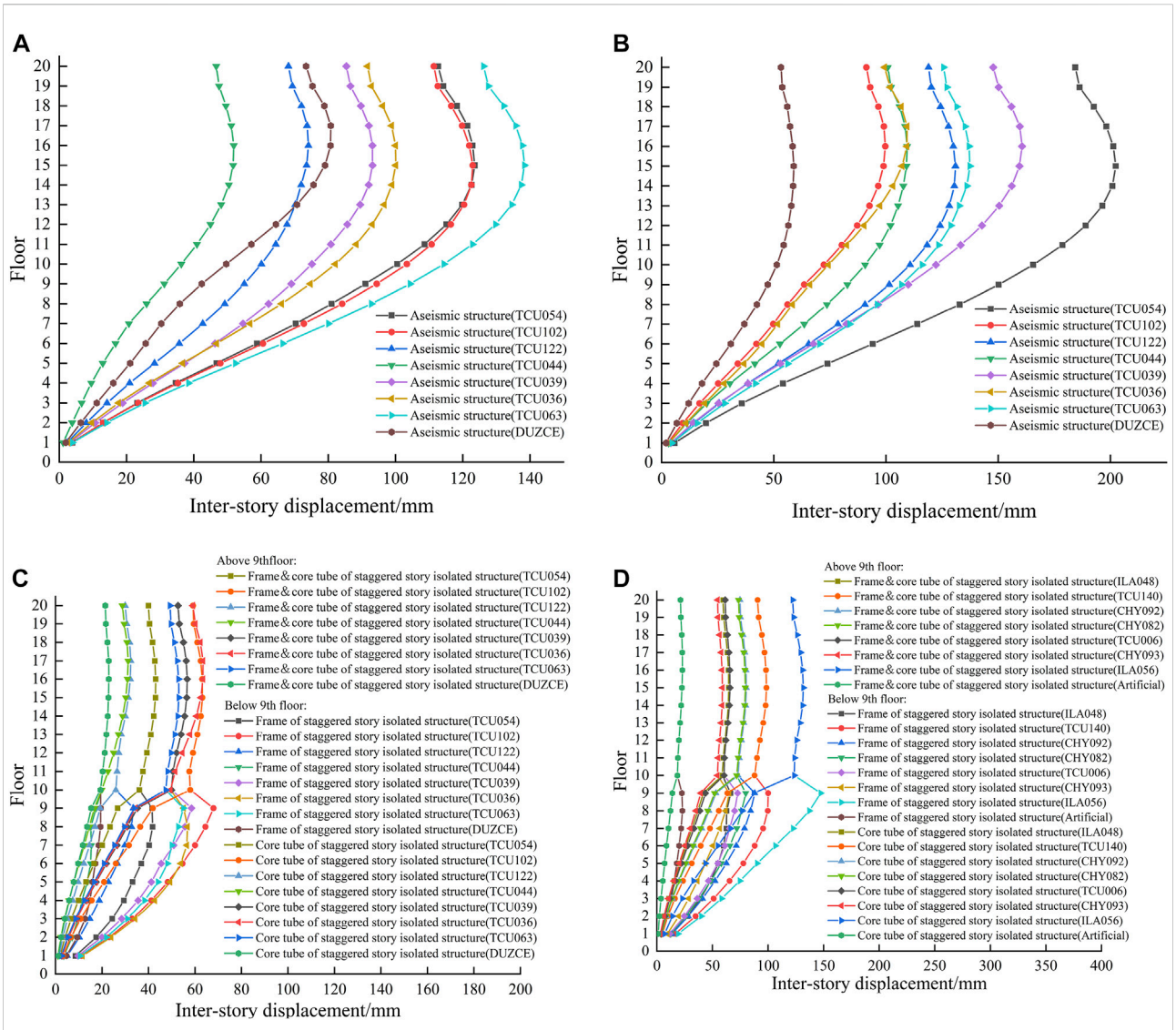

FIGURE 8
Comparisons of inter-story displacement between aeismic structure and new staggered story isolated structure: **(A)** comparison of inter-story displacement of aseismic structure under near-fault pulse-like ground motion **(B)** comparison of inter-story displacement of aseismic structure under far-field harmonic like long-period ground motion, **(C)** comparison of inter-story displacement of new staggered story isolated structure under near-fault pulse-like ground motion, and **(D)** comparison of inter-story displacement of new staggered story isolated structure under far-field harmonic like long-period ground motion.

below the frame isolated layer is greater than that of the frame part. Among them, the inter-layer displacement of the frame component beneath the frame isolated layer is greater than that of the aseismic structure. Under the influence of the far-field harmonic long-period ground motion and near-fault impulse ground motion, the acceleration of the frame part and the acceleration of the core tube part under the frame isolated layer of the new staggered story isolated structure is greater than that of the aseismic structure. The seismic response of aseismic structures in the presence of the far-field harmonic long-period ground motion and near-fault impulse ground motion is greater than that of the ordinary ground motion. The seismic response of the new isolated structure with staggered stories is stronger under the far-field harmonic long-period ground motion and near-fault impulse ground motion is greater than that of the ordinary ground motion. The inter-layer displacement under far-field harmonic like long-period ground motion is greater than that under near-fault pulse long-period ground motion.

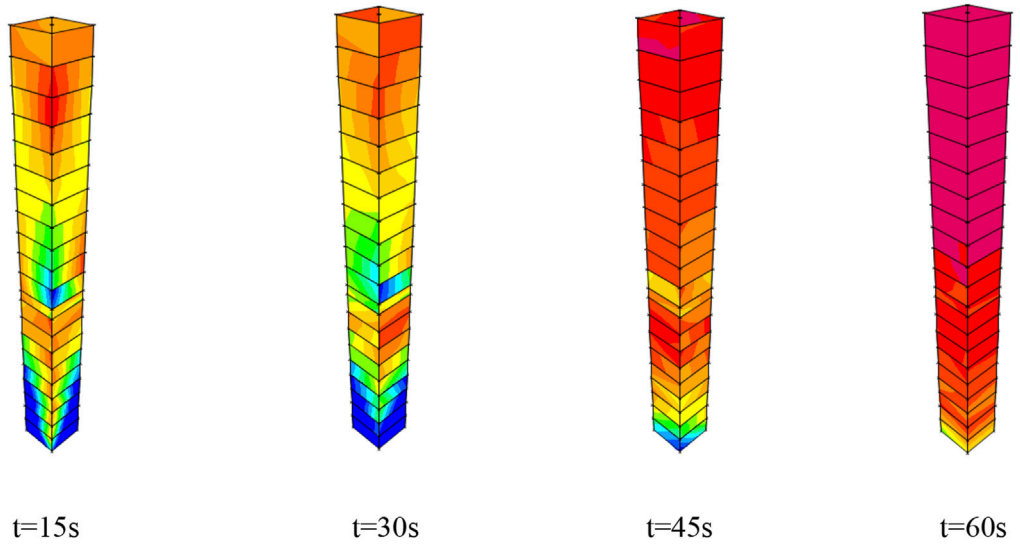

FIGURE 9
Energy time history diagram of a new staggered story isolated structure under ordinary ground motion.

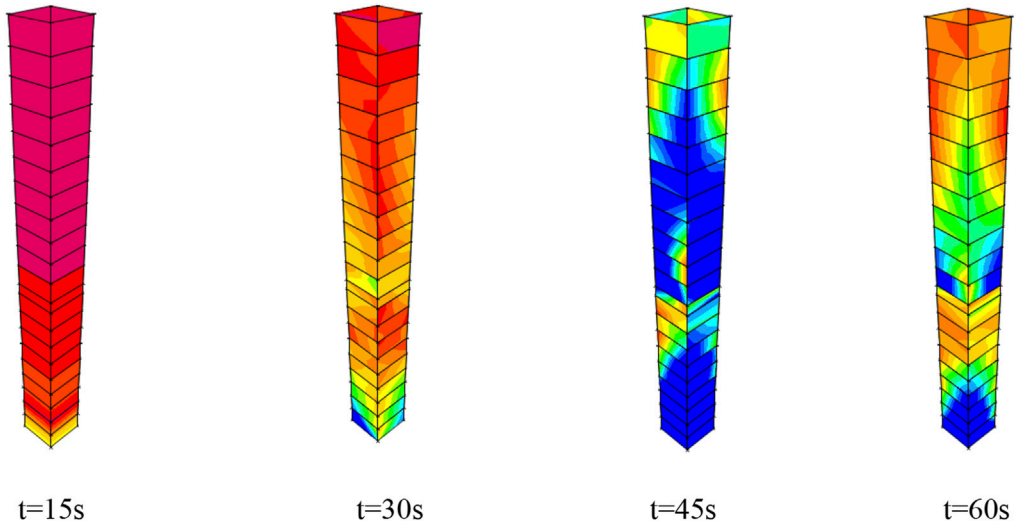

FIGURE 10
Energy time history diagram of a new staggered story isolated structure under near-fault impulse ground motion.

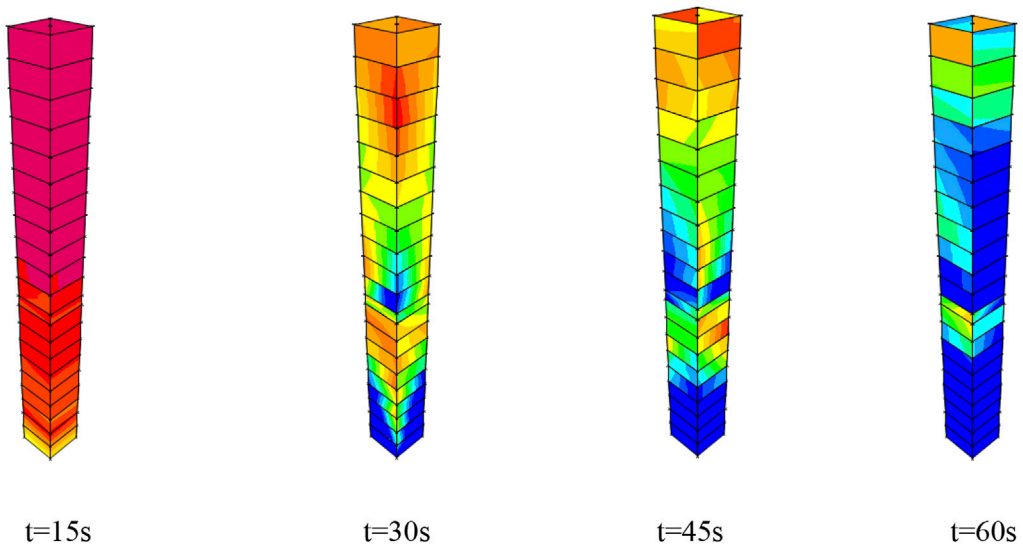

FIGURE 11
Energy time history diagram of a new staggered story isolated structure under far-field harmonic long-period ground motions.

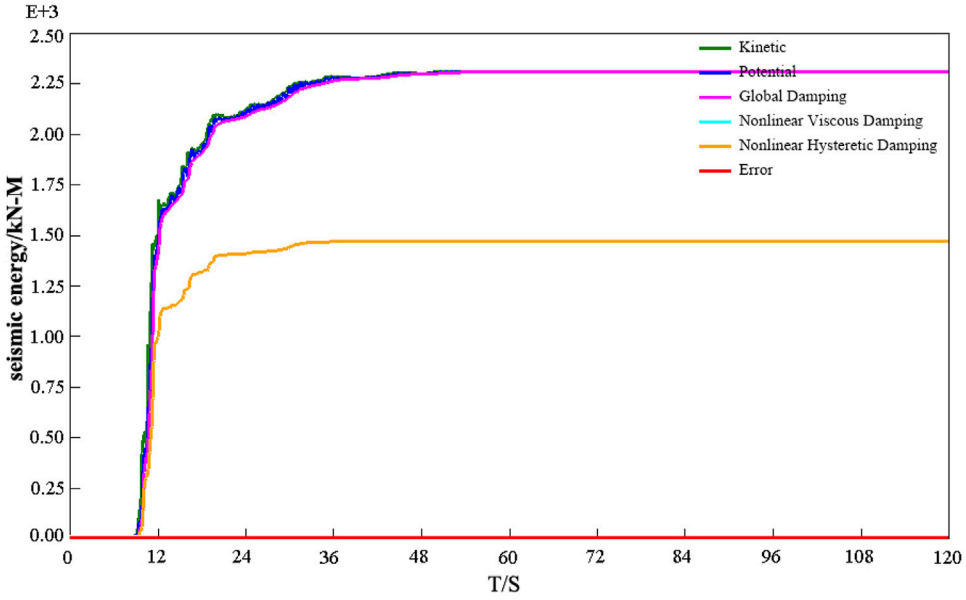

FIGURE 12
Energy time history diagram of a new staggered story isolated structure under ordinary ground motion.

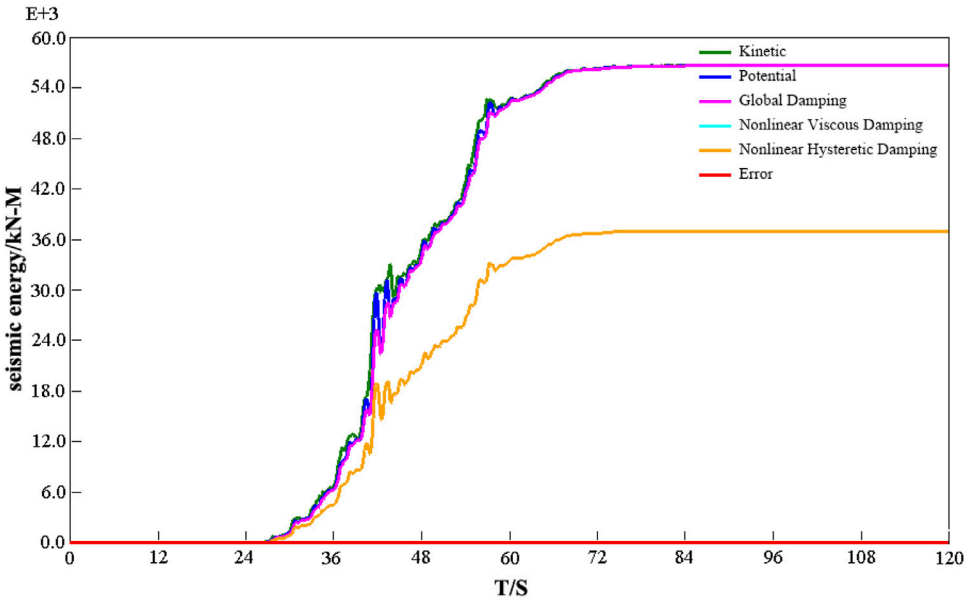

FIGURE 13
Energy time history diagram of a new staggered story isolated structure under near-fault impulse ground motion.

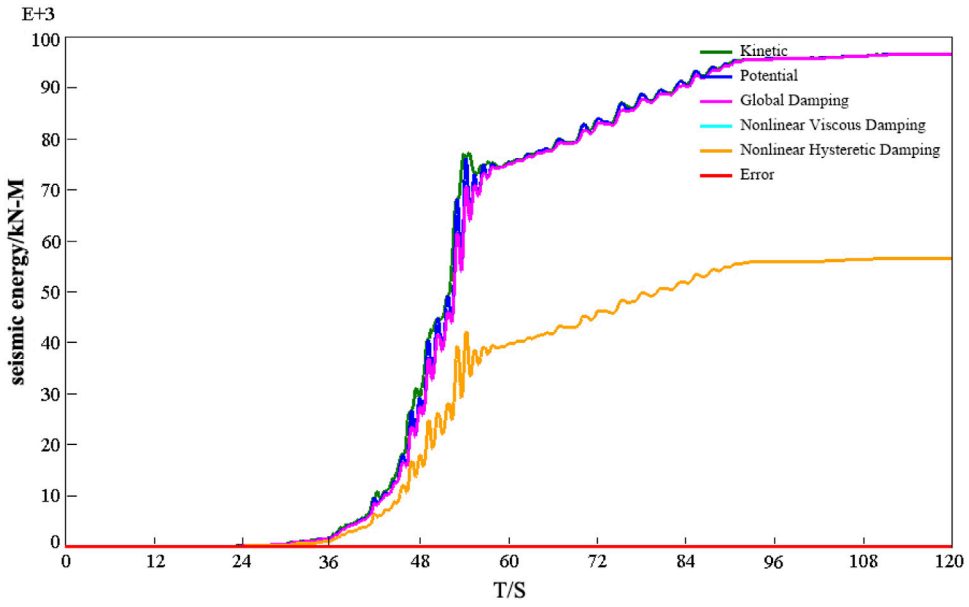

FIGURE 14
Energy time history diagram of a new staggered story isolated structure under far-field harmonic long-period ground motions.

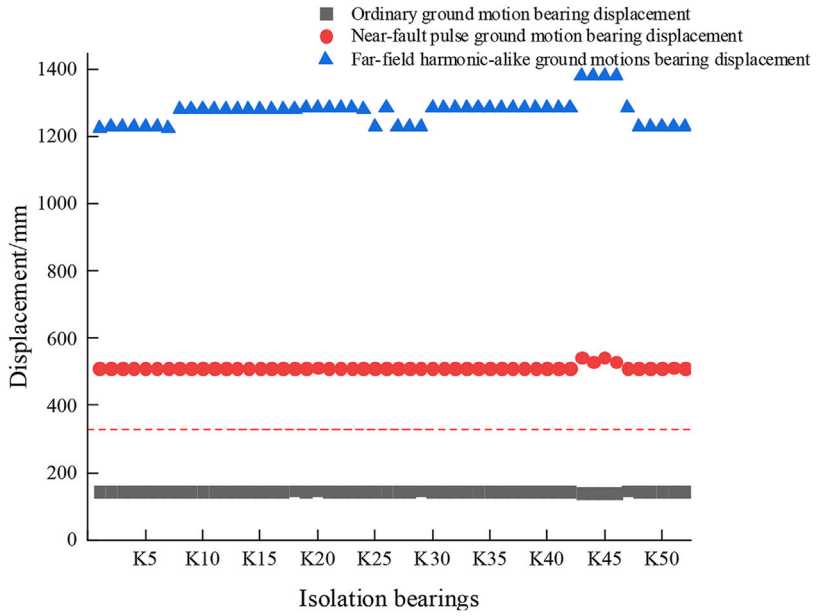

FIGURE 15
Support displacement.

3.2 Damage evolution of structures under different types of ground motions

The damage nephogram of the core tube was retrieved for comparative analysis in order to evaluate the damage evolution of the new staggered story isolated structure under varied ground motions, as well as three different types of ground motions were selected. From Figure 9–11, it can be observed that under the influence of ordinary ground motion, the damage to the bottom of the structure is not obvious, and the majority of the structure is in normal working condition. However, the damage of the core tube caused by far-field harmonic ground motion gradually accumulates over time, extending upward from the base of the structure and producing more damage. It demonstrates that in the middle and later stages of the long-period ground motion, it is simple for structural damage to accumulate.

3.3 Structural energy consumption

From Figures 12–14, it is evident that under the action of three types of ground motions, the input energy, the damping energy consumption, and hysteretic energy consumption of the near-fault pulse type ground motion and the far-field harmonic long-period ground motion grow more rapidly than that of the ordinary ground motion. The energy input of the structure reaches its peak more quickly under the ordinary ground motion, whereas the energy input of the near-fault pulse type ground motion and the far-field harmonic long-period ground motion is more than that of the ordinary ground motion.

Table 5 compares the energy dissipation impact of the new staggered story isolated structure. Under the influence of three different types of seismic waves, it is evident that the new isolated construction with staggered stories has played an effective role in structural energy dissipation. Long-period earthquakes require more attention because the input energy of the near-fault pulse type seismic wave and the far-field harmonic long-period seismic wave is greater than that of the ordinary seismic wave.

4 Response of the isolated bearing

Structural dynamic time history analysis under the peak acceleration of the seismic wave of 400 cm/s^2.

4.1 Maximum displacement of the isolated layer

Under time-history working conditions, the maximum horizontal displacement of the isolated bearing is equal to the envelope value of the three seismic waves. According to the code for seismic design of buildings GB50011-2010, this value cannot exceed the lesser of 0.55 times of the effective diameter or 3 times of the entire thickness of the rubber bearing. In this paper, the

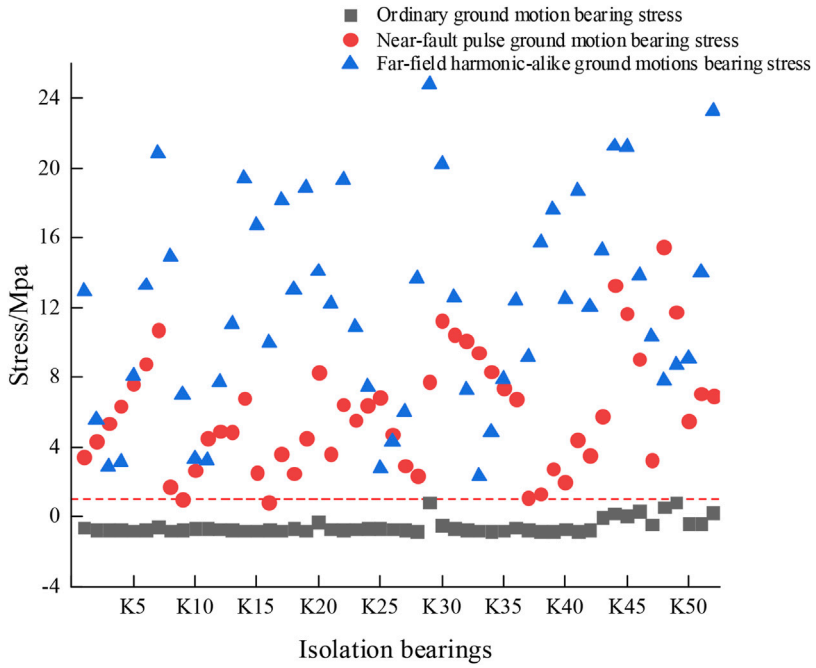

FIGURE 16
Maximum tensile stress of abutment.

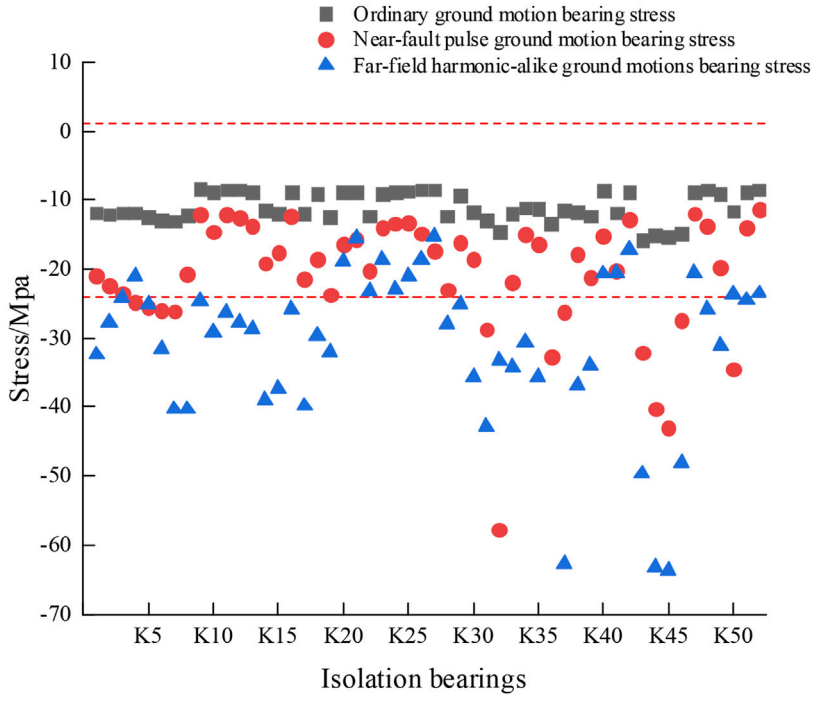

FIGURE 17
Maximum abutment compressive stress.

isolated bearings of LRB600, and LRB1000 are employed, hence the minimum bearing displacement is 600 × 0.55=330 mm.

Define the envelope value of the load combination under seismic working conditions, and extract the envelope value of the horizontal displacement of the isolated bearing under time history working conditions of three distinct types of seismic waves. Figure 15 demonstrates that the bearing displacement under the action of a ordinary seismic wave meets the standard, whereas the bearing displacement under the action of a near-fault layer impulse seismic wave and a far-field harmonic long-period seismic wave significantly exceeds the standard value.

4.2 Tensile stress of isolated bearing

In accordance with the provisions on the maximum tensile stress limit value of the rubber isolated bearing in article 12.2.4 of the code for seismic resistance, the tensile stress of the isolated bearing must not exceed 1 MPa during earthquakes. Figure 16 depicts the pressure for computing the minimal surface pressure. It can be seen from Figure 16 that among the time history conditions of three different types of seismic waves, the maximum tensile stress of the bearing under the action of the ordinary seismic wave meets the requirements, whereas the maximum tensile stress of the bearing under the action of the far-field harmonic long-period seismic wave and the near-fault pulse type seismic wave exceeds the limit.

4.3 Check the compressive stress of the isolated bearing

In general, 2 times of the reference surface pressure can be used as the limit for the maximum surface pressure of the bearing. The structure described in this study is a class B structure, hence the reference surface pressure is 12 MPa, and the limit value of the maximum surface pressure is 24 MPa. Figure 17 illustrates the calculated value of the maximum surface pressure of the bearing and reveals that under the influence of three distinct types of seismic waves, the maximum compressive stress of the bearing under the action of the ordinary seismic wave satisfies the requirements of the specification, whereas the majority of the maximum compressive stress of the bearing under the influence of the far-field harmonic long-period seismic wave and the near-fault impulse seismic wave exceeds the limit.

5 Discussion

In this paper, the finite element analysis software ETABS is used to analyze the long-period seismic response of a new staggered story isolated structure. The seismic response analysis and the damage of the seismic structure are investigated from the perspectives of the seismic wave selection, damping effect index, structural damage, energy dissipation, and the response of the isolated bearings. Under the long-period ground motion, it is concluded that the new staggered story isolated structure has a good seismic isolated effect.

Through the research of this paper, further research can be carried out in the following aspects:

(1) In this paper, the seismic response analysis of the new staggered story isolated structure under different types of the ground motion input is primarily based on numerical analysis, Sugimoto et al. (2016) and different parameter settings may lead to certain errors in the results. To verify the analysis results presented in this paper, shaking table tests with the input of the long-period ground motion can be carried out in the future.

(2) Currently, the majority of studies focuses on the base foundation isolated structures and the mid-story isolated structures (Bhandari et al., 2019; Faiella and Mele, 2020) Few studies have been conducted on the new staggered story isolated structure, and the response of this structure to long-period ground motion has also received little attention. This paper reveals that the new staggered story isolated structure has a good shock absorption effect under the action of the long-period ground motion, but that structural damage and bearing overrun are significant under the long-period action.

(3) The largest isolated bearing employed in this paper has a 1000 mm diameter. It remains to be determined if the damage to the core tube, the maximum tensile stress, and the maximum compressive stress of the isolated bearings can be reduced by increasing the diameter and altering the layout of the isolated bearings beneath the core tube (Fakih et al., 2021; Thakur et al., 2021).

(4) The influence of the vertical ground motion on the structure is not examined in this research (Quaranta et al., 2022; Wang et al., 2022). In fact, seismic waves are multi-dimensional. If some of these factors are disregarded, the result of the shock absorption effect may be deviated. At present, there are a few studies on this topic, and the follow-up research can be expanded using the new staggered story isolated structure.

(5) In this paper, the seismic response analysis of the structure is performed with a rigid foundation assumption. In practice, the interaction between the structure and soil presents a challenge. Domestic and international scholars have conducted numerous studies on this issue. No uniform result has been reached as to whether the interaction effect of soil and structure on the seismic response of an isolated structure is increased or decreased (Askouni and Karabalis, 2022; Zhang and Far, 2022). The interaction between soil and structure in

high-rise seismically isolated structures subjected to long-period ground motion has not yet been investigated.

(6) From a vast amount of seismic data for a particular ground motion, long-period seismic activity is selected and input into the structure for seismic response analysis (Shuoyu et al., 2021) However, the seismic response study must include both natural and artificial waves, as required by the applicable analysis. Therefore, it is necessary to investigate the theoretical basis and synthesis method of the artificial combination of long-period seismic waves.

6 Conclusion

In this paper, the seismic response models of the aseismic structure and the new staggered story isolated structure are developed. Three forms of ground motions are input into the nonlinear response analysis, and the discrepancies between the seismic response laws of this two kinds of stucture under different ground motions are explored. The following conclusions are obtained:

(1) Compared to the aseismic structure, the new staggered story isolated structure has a greater effect on shock absorption when subjected to three distinct types of seismic waves.

(2) There are certain differences in the shock absorption effect under the three kinds of ground motions; The seismic response under ordinary ground motions is smaller, whereas the seismic response under the near-field harmonic long-period ground motion and the near-field fault pulse type earthquake are larger; Meanwhile, the inter story shear force, inter story acceleration and inter-story displacement are increased. Therefore, the damage and the energy input are also increased.

(3) Under rare earthquakes, the isolated bearing is in good condition under the ordinary ground motion. However, the bearing exceeds its limit under near-fault impulse ground motion and far-field harmonic and long-period earthquakes. Consequently, special attention should be given to the region where the far-field harmonic and long-period ground motion are involved.

Data availability statement

The raw data supporting the conclusion of this article will be made available by the authors, without undue reservation.

Author contributions

All authors listed have made a substantial, direct, and intellectual contribution to the work and approved it for publication.

Conflict of interest

Author ZG was employed by the company Shandong Jining Wenshang County Architectural Design Institute Co., Ltd.

The remaining authors declare that the research was conducted in the absence of any commercial or financial relationships that could be construed as a potential conflict of interest.

Publisher's note

All claims expressed in this article are solely those of the authors and do not necessarily represent those of their affiliated organizations, or those of the publisher, the editors and the reviewers. Any product that may be evaluated in this article, or claim that may be made by its manufacturer, is not guaranteed or endorsed by the publisher.

References

Ali, A., Zhang, C. W., Bibi, T., Zhu, L. M., Cao, L. Y., Li, C. X., et al. (2022). Investigation of five different low-cost locally available isolation layer materials used in sliding base isolation systems. *Soil Dyn. Earthq. Eng.* 154, 107127–127. doi:10.1016/j.soildyn.2021.107127

Askouni, P., and Karabalis, D. (2022). The modification of the estimated seismic behaviour of r/c low-rise buildings due to ssi. *Buildings* 127, 975. doi:10.3390/buildings12070975

Behzad Talaeitaba, S., Safaie, M., and Zamani, R. (2021). Development and application of a new base isolation system in low-rise buildings. *Structures* 34, 1684–1709. doi:10.1016/j.istruc.2021.07.077

Bhandari, M., Bharti, S. D., Shrimali, M., and Datta, T. (2019). Seismic fragility analysis of base-isolated building frames excited by near-and far-field earthquakes. *J. Perform. Constr. Facil.* 33, 1–16. doi:10.1061/(asce)cf.1943-5509.0001298

Cancellara, D., and De Angelis, F. (2016). Nonlinear dynamic analysis for multi-storey rc structures with hybrid base isolation systems in presence of bi-directional ground motions. *Compos. Struct.* 154, 464–492. doi:10.1016/j.compstruct.2016.07.030

Castaldo, P., and Tubaldi, E. (2018). Influence of ground motion characteristics on the optimal single concave sliding bearing properties for base-isolated structures. *Soil Dyn. Earthq. Eng.* 104, 346–364. doi:10.1016/j.soildyn.2017.09.025

Chang, P., and Zhu, J. (2011). Seismic vulnerability analysis of mid-story isolation and reduction structures based stochastic vibration. *Adv. Mat. Res.* 243-249, 3988–3991. doi:10.4028/www.scientific.net/amr.243-249.3988

Chang, Z., Catani, F., Huang, F., Liu, G., Meena, S. R., Huang, J., et al. (2022). Landslide susceptibility prediction using slope unit-based machine learning models considering the heterogeneity of conditioning factors. *J. Rock Mech. Geotechnical Eng.* doi:10.1016/j.jrmge.2022.07.009

Chang, Z., Du, Z., Zhang, F., Huang, F., Chen, J., Li, W., et al. (2020). Landslide susceptibility prediction based on remote sensing images and gis: Comparisons of

supervised and unsupervised machine learning models. *Remote Sens.* 12, 502. doi:10.3390/rs12030502

Cheng, Y., Dong, Y. R., Qin, L., Wang, Y. Y., and Li, Y. X. (2021). Seismic energy response of sdof systems subjected to long-period ground motion records. *Adv. Civ. Eng.* 2021, 1–20. doi:10.1155/2021/6655400

Clemente, P., Di Cicco, A., Saitta, F., and Salvatori, A. (2021). Seismic behavior of base isolated civil protection operative center in Foligno, Italy. *J. Perform. Constr. Facil.* 35 (4), 04021027. doi:10.1061/(asce)cf.1943-5509.0001589

Davas, S., Temür, R., and Alhan, C. (2022). Comparison of meta-heuristic approaches for the optimization of non-linear base-isolation systems considering the influence of superstructure flexibility. *Eng. Struct.* 263, 114347. doi:10.1016/j.engstruct.2022.114347

De Luca, A., and Guidi, L. G. (2019). State of art in the worldwide evolution of base isolation design. *Soil Dyn. Earthq. Eng.* 125, 105722. doi:10.1016/j.soildyn.2019.105722

Erdik, M., Ulker, O., Sadan, B., and Tuzun, C. (2018). Seismic isolation code developments and significant applications in Turkey. *Soil Dyn. Earthq. Eng.* 115, 413–437. doi:10.1016/j.soildyn.2018.09.009

Faiella, D., Calderoni, B., and Mele, E. (2020). Seismic retrofit of existing masonry buildings through inter-story isolation system: A case study and general design criteria. *J. Earthq. Eng.* 26, 2051–2087. doi:10.1080/13632469.2020.1752854

Faiella, D., and Mele, E. (2020). Insights into inter-story isolation design through the analysis of two case studies. *Eng. Struct.* 215, 110660. doi:10.1016/j.engstruct.2020.110660

Fakih, M., Hallal, J., Damerji, H., and Darwich, H. (2021). Effect of lead-rubber bearing isolators in reducing seismic damage for a high-rise building in comparison with normal shear wall system. *Struct. Durab. Health Monit.* 15, 247–260. doi:10.32604/sdhm.2021.015174

Forcellini, D., and Gallanti, L. (2018). Seismic assessment of storey isolation on tall buildings. *Innov. Infrastruct. Solut.* 3 (1), 58–15. doi:10.1007/s41062-018-0163-2

Fu, W. Q., Zhang, C. W., Li, M., and Duan, C. K. (2019). Experimental investigation on semi-active control of base isolation system using magnetorheological dampers for concrete frame structure. *Appl. Sci. (Basel).* 918, 3866. doi:10.3390/app9183866

Guo, Z. Z., Shi, Y., Huang, F. M., Fan, X. M., and Huang, J. S. (2021). Landslide susceptibility zonation method based on c5.0 decision tree and k-means cluster algorithms to improve the efficiency of risk management. *Geosci. Front.* 12, 101249. doi:10.1016/j.gsf.2021.101249

Guo, Z., Chen, L., Gui, L., Du, J., Yin, K., and Do, H. M. (2020a). Landslide displacement prediction based on variational mode decomposition and WA-GWO-BP model. *Landslides* 17 (3), 567–583. doi:10.1007/s10346-019-01314-4

Guo, Z., Chen, L., Yin, K., Shrestha, D. P., and Zhang, L. (2020b). Quantitative risk assessment of slow-moving landslides from the viewpoint of decision-making: A case study of the three gorges reservoir in China. *Eng. Geol.* 273, 105667. doi:10.1016/j.enggeo.2020.105667

Hayashi, K., Fujita, K., Tsuji, M., and Takewaki, I. (2018). A simple response evaluation method for base-isolation building-connection hybrid structural system under long-period and long-duration ground motion. *Front. Built Environ.* 4, 2. doi:10.3389/fbuil.2018.00002

Hu, R. P., Xu, Y. L., and Zhao, X. (2018). Long-period ground motion simulation and its impact on seismic response of high-rise buildings. *J. Earthq. Eng.* 22, 1285–1315. doi:10.1080/13632469.2017.1286617

Huang, F., Cao, Z., Guo, J., Jiang, S-H., Li, S., and Guo, Z. (2020a). Comparisons of heuristic, general statistical and machine learning models for landslide susceptibility prediction and mapping. *CATENA* 191, 104580. doi:10.1016/j.catena.2020.104580

Huang, F., Cao, Z., Jiang, S-H., Zhou, C., Huang, J., and Guo, Z. (2020b). Landslide susceptibility prediction based on a semi-supervised multiple-layer perceptron model. *Landslides* 1712, 2919–2930. doi:10.1007/s10346-020-01473-9

Huang, F., Chen, J., Liu, W., Huang, J., Hong, H., and Chen, W. (2022). Regional rainfall-induced landslide hazard warning based on landslide susceptibility mapping and a critical rainfall threshold. *Geomorphology* 408, 108236. doi:10.1016/j.geomorph.2022.108236

Huang, F., Zhang, J., Zhou, C., Wang, Y., Huang, J., and Zhu, L. (2020c). A deep learning algorithm using a fully connected sparse autoencoder neural network for landslide susceptibility prediction. *Landslides* 17, 217–229. doi:10.1007/s10346-019-01274-9

Hur, M. W., and Park, T. W. (2022). Seismic performance of story-added type buildings remodeled with story seismic isolation systems. *Buildings* 12, 270. doi:10.3390/buildings12030270

Jiang, S-H., Huang, J., Huang, F., Yang, J., Yao, C., and Zhou, C. (2018). Modelling of spatial variability of soil undrained shear strength by conditional random fields for slope reliability analysis. *Appl. Math. Model.* 63, 374–389. doi:10.1016/j.apm.2018.06.030

Jose, S. K., Anjali, G. S., Nair, A. S., Adithya, D. A., Sony, A., and Arunima, A. S. (2021). Fixed and base isolated framed structures: A comparative study. *J. Phys. Conf. Ser.* 2070, 012198. doi:10.1088/1742-6596/2070/1/012198

Kamble, V., Dayal Bharti, S., Kumar Shrimali, M., and Kanti Datta, T. (2022). Control of secondary systems response in a base-isolated building under tridirectional ground motion. *Pract. Period. Struct. Des. Constr.* 27, 04021060. doi:10.1061/(asce)sc.1943-5576.0000641

Li, W., Wang, S., Miao, Q., and Liu, J. (2014). Nonlinear stimulation of reinforced masonry structure and adding-story isolation model. *China Civ. Eng. J.* 47, 35–40.

Li, Z. H., Huang, G. Q., Chen, X. Z., and Zhou, X. H. (2022). Seismic response and parametric analysis of inter-story isolated tall buildings based on enhanced simplified dynamic model. *Int. J. Str. Stab. Dyn.* 22. doi:10.1142/s0219455422400089

Liao, W. I., Loh, C. H., and Wan, S. (2001). Earthquake responses of rc moment frames subjected to near-fault ground motions. *Struct. Des. Tall Build.* 10, 219–229. doi:10.1002/tal.178

Liu, D., Li, L., Zhang, Y., Chen, L., Wan, F., and Yang, F. (2022). Study on seismic response of a new staggered story isolated structure considering SSI effect. *J. Civ. Eng. Manag.* 28 (5), 397–407. doi:10.3846/jcem.2022.16825

Liu, F., Zhang, S., Hu, Y., Li, S., and Zhu, L. (2021). Study on seismic response characteristics of the interlayer isolation structure. *J. Vibroeng.* 23, 1765–1784. doi:10.21595/jve.2021.22003

Liu, Y. H., Wu, J. B., and Dona, M. (2018). Effectiveness of fluid-viscous dampers for improved seismic performance of inter-storey isolated buildings. *Eng. Struct.* 169, 276–292. doi:10.1016/j.engstruct.2018.05.031

Loh, C. H., Weng, J. H., Chen, C. H., and Lu, K. C. (2013). System identification of mid-story isolation building using both ambient and earthquake response data. *Struct. Control Health Monit.* 202, 139–155. doi:10.1002/stc.479

Losanno, D., Ravichandran, N., Parisi, F., Calabrese, A., and Serino, G. (2021). Seismic performance of a low-cost base isolation system for unreinforced brick masonry buildings in developing countries. *Soil Dyn. Earthq. Eng.* 141, 106501. doi:10.1016/j.soildyn.2020.106501

Ma, X. T., Bao, C., Shu Ing, D., Lu, H., Zhang, L. X., Ma, Z. W., et al. (2020). Dynamic response analysis of story-adding structure with isolation technique subjected to near-fault pulse-like ground motions. *Phys. Chem. Earth, Parts A/B/C* 121, 102957. doi:10.1016/j.pce.2020.102957

Mashinskii, E. I. (2019). Effects of intermittent inelasticity when propagating seismic wave in low velocity zone. *Gorn. Nauki. Tehnol.* 4, 31–41. doi:10.17073/2500-0632-2019-1-31-41

Minagawa, K., and Fujita, S. (2006). Fundamental study on the super-long-period active isolation system. *J. Press. Vessel Technol.* 128, 502–507. doi:10.1115/1.2349555

Park, W., and Ok, S. Y. (2021). Hybrid optimization design approach of asymmetric base-isolation coupling system for twin buildings. *J. Low Freq. Noise Vib. Act. Control* 40, 1993–2013. doi:10.1177/1461348421992969

Pérez-Rocha, L. E., Avilés-López, J., and Tena-Colunga, A. (2021). Base isolation for mid-rise buildings in presence of soil-structure interaction. *Soil Dyn. Earthq. Eng.* 151, 106980. doi:10.1016/j.soildyn.2021.106980

Pytel, W., Świtoń, J., and Wójcik, A. (2016). The effect of mining face's direction on the observed seismic activity. *Int. J. Coal Sci. Technol.* 3, 322–329. doi:10.1007/s40789-016-0122-5

Qahir Darwish, A., and Bhandari, M. (2022). Seismic response reduction of high rise steel-concrete composite buildings equipped with base isolation system. *Mater. Today Proc.* 59, 516–524. doi:10.1016/j.matpr.2021.11.560

Quaranta, G., Angelucci, G., and Mollaioli, F. (2022). Near-fault earthquakes with pulse-like horizontal and vertical seismic ground motion components: Analysis and effects on elastomeric bearings. *Soil Dyn. Earthq. Eng.* 160, 107361. doi:10.1016/j.soildyn.2022.107361

Rostami, A., and Poursha, M. (2021). A lateral load distribution for the static analysis of base-isolated building frames under the effect of far-fault and near-fault ground motions. *Structures* 34, 2384–2405. doi:10.1016/j.istruc.2021.08.125

Saha, A., and Mishra, S. K. (2021). Implications of inter-storey-isolation (isi) on seismic fragility, loss and resilience of buildings subjected to near fault ground motions. *Bull. Earthq. Eng.* 20, 899–939. doi:10.1007/s10518-021-01277-9

Shan, J. Z., Shi, Z. G., Gong, N., and Shi, W. X. (2020). Performance improvement of base isolation systems by incorporating eddy current damping and magnetic spring under earthquakes. *Struct. Control Health Monit.* 27 (6), e2524. doi:10.1002/stc.2524

Shang, S. P., and Hu, L. H. (2020). Analysis of energy dissipation characteristics of base isolation structures. *Earthq. Eng. Eng. Dyn.* 40.1, 12–21.

Shuoyu, L., Jiang, Y., Li, M., Xin, J., and Peng, L. (2021). Long period ground motion simulation and its application to the seismic design of high-rise buildings. *Soil Dyn. Earthq. Eng.* 143, 106619. doi:10.1016/j.soildyn.2021.106619

Sugimoto, K., Yonezawa, K., Katsumata, H., and Fukuyama, H. (2016). Shaking table test of quarter scale 20 story rc moment frame building subjected to long period ground motions. *J. Disaster Res.* 11, 97–105. doi:10.20965/jdr.2016.p0097

Thakur, R., Al Agha, W., Thakur, M., and Umamaheswari, N. (2021). Impact of the lead rubber base isolators on reinforced concrete building. *IOP Conf. Ser. Mater. Sci. Eng.* 1026 (1). doi:10.1088/1757-899X/1026/1/012004

Van-Thuyet, N. (2021). Effectiveness of base-isolated low-rise masonry building under ex-citation from earthquakes. *Mag. Civ. Eng.* 8 (108), 10803.

Wang, R., Zhu, T., Yu, J-K., and Zhang, J-M. (2022). Influence of vertical ground motion on the seismic response of underground structures and underground-aboveground structure systems in liquefiable ground. *Tunn. Undergr. Space Technol.* 122, 104351. doi:10.1016/j.tust.2021.104351

Wu, Y. X., Dong, X. J., Lin, Y. Q., and Cheng, H. D. (2022). Field test for a base isolation structure on condition of horizontal and initial displacement. *Appl. Sci.* 12 (1), 232. doi:10.3390/app12010232

Zhang, X., and Far, H. (2022). Effects of dynamic soil-structure interaction on seismic behaviour of high-rise buildings. *Bull. Earthq. Eng.* 20, 3443–3467. doi:10.1007/s10518-021-01176-z

Zhang, Y., Liu, D., Fang, S., Lei, M., Zhu, Z., and Liao, W. (2022). Study on shock absorption performance and damage of a new staggered story isolated system. *Adv. Struct. Eng.* 25 (5), 1136–1147. doi:10.1177/13694332211056113

Zhou, J., Jiang, Y., Wang, L. X., and Fang, X. D. (2018). A long-period elastic response spectrum based on the site-classification of Chinese seismic code. *Soil Dyn. Earthq. Eng.* 115, 622–633. doi:10.1016/j.soildyn.2018.09.024